International Journal of Enhanced Research in Science Technology & Engineering, ISSN: 2319-7463
Vol. 3 Issue 11, November-2014, pp: (123-130), Impact Factor: 1.252, Available online at: www.erpublications.com

Hydrothermal Synthesis of TiO_2 Nanorods using $TiCl_3$ and Its Gas Sensing Properties

Ganesh J. Mogal[1], Daga V. Ahire[1], G. E. Patil[2], Gotan H. Jain[2*], V. B. Gaikwad[3]
[1]Materials Research Lab, K.T.H.M. College, Nashik 422013, India
[2]Department of Physics, SNJBs K.K.H.A. Arts, S.M.G.G.L. Commerce and Science College, Chandwad 423101
[3]Director, BCUD, Savitribai Phule Pune University, Pune 411007

Abstract: TiO_2 nanorods have been successfully obtained with hydrothermal method by treating $TiCl_3$ with NaOH and NaCl aqueous solution at 180°C for 24h in an autoclave. The present investigation deals with the preparation of TiO_2 nanorods and gas sensing performance of TiO_2 based thick film resistors. The Thick films of synthesised material were prepared by screen-printing technique. The thick films were characterized for X-Ray diffraction (XRD), Scanning electron microscopy (SEM), UV visible spectroscopy and Transmission electron microscopy (TEM) and SAED. TiO_2 thick film gives high sensitivity and selectivity for H_2S gas. The reasons behind the higher sensitivity are interpreted.

Keywords: TiO_2 nanorods; hydrothermal synthesis; thick films; gas sensor; screen-printing technique.

Introduction

Conductometric metal oxide sensors comprise a significant part of the gas sensor components markets. Metal oxide sensors remain a widely used choice for range of gas species[1-7] These devices offers low cost, high sensitivity, fast response and relative simplicity, advantages that should work in their favor as new application emerge, especially in the field of portable devices. The working principle of a typical resistive metal oxide gas sensor is based on a shift of the equilibrium of the surface oxygen reaction due to the presence of the target analyte. The change in concentration of adsorbed oxygen changes resistance of gas sensing material.

The structural parameters of metal oxides controlling gas sensing effects are thickness of films, grain size, porosity, grain faceting, agglomeration, film texture, surface geometry, sensor geometry, surface disordering, bulk stoichiometry, grain network, active surface area and size of necks. The different synthesis methods for TiO_2 Nanostructure are Sol-Gel method, Solvothermal method, direct oxidation method, hydrothermal method and Microwave method. Hydrothermal research was initiated in the middle of the 19th century by geologists and was aimed at laboratory simulations of natural hydrothermal phenomena. In the 20th century, hydrothermal synthesis was clearly identified as an important technology for materials synthesis, predominantly in the fields of hydrometallurgy and single crystal growth. However, the severe (supercritical) reaction conditions required particularly for growing single crystals have discouraged extensive research and commercialization for many materials.

Hydrothermal synthesis is a method of synthesis of single crystal that depends on the solubility of minerals in hot water under high pressure. The crystal growth is performed in an apparatus consisting of a steel pressure vessel called autoclave, in which a nutrient is supplied along with water. A gradient of temperature is maintained at the opposite ends of the growth chamber so that the hotter end dissolves the nutrient and the cooler end causes seeds to take additional growth. The advantages of the hydrothermal method over other types are Crystal growth includes the ability to create crystalline phases which are not stable at the melting point. Materials which have a high vapor pressure near their melting points can also be grown by the hydrothermal method. This method is also particularly suitable for the growth of large good-quality crystals while maintaining good control over their composition.

In recent years, interest has grown in the development of an “electronic nose," capable of detecting mixed gases and even odors. Instead of analyzing all of the gas constituents by a technique such as gas chromatography, an electronic nose looks for specific patterns or fingerprints of the gas mixture. Such a device generally consists of chemical sensors, each one sensitive to a specific gas and a pattern recognition system. There are three basic types of sensors i.e. solid electrolyte sensors, catalytic sensors and semi-conducting oxide gas sensors. The widely used type of gas sensor is effectively a semi-conducting oxide gas sensor. Because of their simplicity and low cost, semiconductor metal-oxide gas sensors stand out among the ones used in multi-sensor arrays. A multi-sensor array has been proposed for environmental monitoring, in which gas sensing would be based on changes in the surface or near-surface oxide conductivity.
Two of the most important issues in gas sensing devices are gas sensitivity (detection of gas concentrations at the ppm level) and gas selectivity (detection of specific gases in a mixed gas environment). Semiconductor oxides suffer mostly

from a lack of gas selectivity. For instance, the most commonly used oxide, TiO_2, can be sensitized to different gases by judicious choice of operating temperature, microstructural modification, and by the use of dopants and catalysts. Nanostructured materials present new opportunities for enhancing the properties and performance of gas sensors because of the much higher surface-to-bulk ratio in nanomaterials compared to coarse micrograined materials.

TiO_2, a low-cost n-type semiconductor, has been of wide interest because of its versatile applications in area such as photocatalysis,dye-sensitized solar cells, sensors[8,9] and self-cleaning coatings. As band gap of anatase TiO_2 is in the near-UV range of the electromagnetic spectrum, Tang et al. [10-12] have studied the behaviour of anatase TiO_2 thin film sensors and found their properties quite different from those of the extensively studied and used rutile phase. TiO_2 crystlizes in three modifications of rutil, anatase and brookite.

Presently the atmospheric pollution has become a global issue. Gases from auto and industrial exhausts are polluting the environment. The reducing gases such as: CO [13], H_2 [14], oxygenic gases such as: CO_2 [15], NOx [16], odorous gases such as: NH_3 , H_2S [17], explosive gases such as: C_3H_8 ,LPG [18] and, toxic gases such as: Cl_2, NO_2 [19] etc. have to be controlled for the healthy survival of the living beings. Thus, there is an increasing concern about minimization of the emission of autointoxication and also to reduce emission of such unburnt hydrocarbons from automobile and industrial exhausts. Thus the need to monitor and control these gases has led to the research and development of a variety of sensors using different materials and technologies.

Experimental

The TiO_2 nanorods were synthesized by a hydrothermal method using $TiCl_3$.30 ml aqueous solution of titanium trichloride ($TiCl_3$, 15% in HCl), sodium chloride (NaCl, 5M and 10M) and sodium hydroxide NaOH (10M) dispread in 130 ml of H_2O.The solutions were stirred at room temperature for 20 min. The mixture was put into a Teflon-lined stainless autoclave which was heated at 180^{o}C for 12h.and it was naturally cooled to room temperature. A white precipitation was filtered and washed with 1 M, HCl and deionized water.

The thixotropic paste [20-23] was formulated by mixing the fine synthesized powder of TiO_2 with solution of ethyl cellulose (as temporary binder) and organic solvents. The paste was screen printed on glass substrate in desired patterns; the prepared films were fired at 550^{o}C for 30 min.

The sensing performance of the thick films was examined by using a static gas sensing system [24, 25]. To heat the sample up to required operating temperatures, the heater is fixed on the base plate. A thermocouple is connected to a digital temperature indicator for temperature measurement. The required gas concentration inside the static system has achieved by injecting a known volume of test gas using a gas-injecting syringe.

Results and Discussion

A. X-ray Diffrcation Analysis

Figure1 shows the XRD pattern, well matching with PDF 01-075-6444 data [26]. The % crystillinity is 76.4%. The average grain size has been estimated as 32.45nm.
Figure 2 shows the pattern, well matching with PDF 00-034-0180 data [27]. The sharp pecks indicate that TiO_2 is well crystalline; the % crystillinity is 75.3%. The average grain size has been estimated as 55.75 nm.

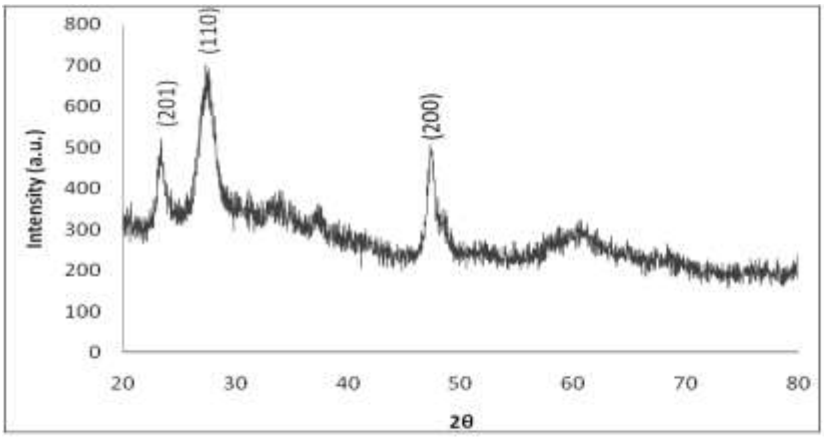

Figure 1: X-Ray diffraction of hydrothermally synthesized (using 5M NaCl) TiO_2 powder.

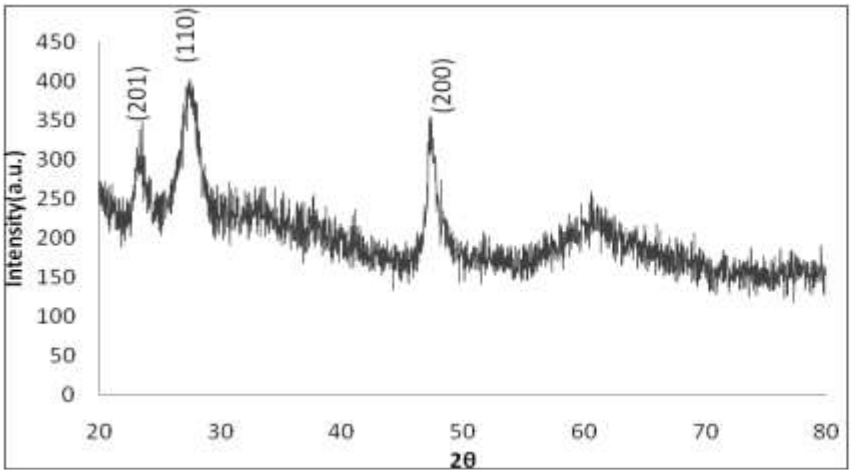

Figure 2. X-Ray diffraction of hydrothermally synthesized (using 10M NaCl) TiO_2 powder.

B. UV-visible Absorption Spectroscopy Analysis

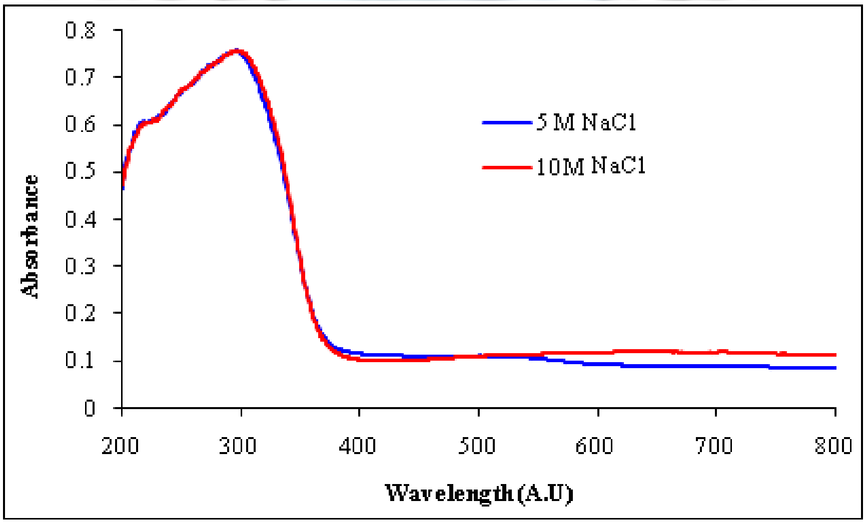

Figure 3. UV-visible absorption spectra of TiO_2

Figure 3 shows UV-visible absorption spectra of TiO_2. It indicates that the band gap of TiO_2 is 4.1eV and 4.0eV for 5M NaCl and 10M NaCl respectively.

C. SEM Analysis

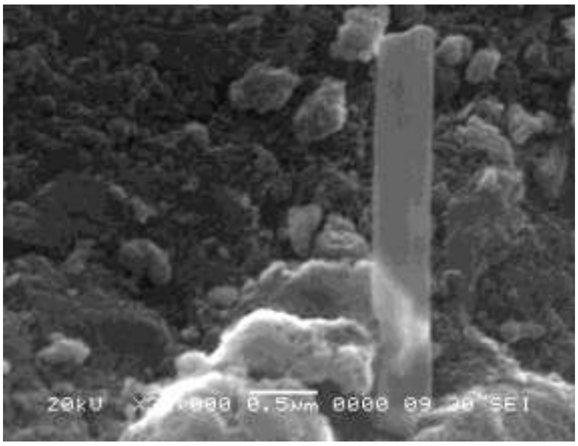

Figure 4. SEM image of hydrothermally synthesized (using 5M NaCl) TiO_2 thick film

The micro structural and chemical compositions of the films were analyzed using a scanning electron microscope (SEM, JEOL JED 6300) coupled with an energy dispersive spectrometer (EDS, JEOL JED 2300LA).Figure .4 shows TiO_2 nanorods of diameter 0.3µm.

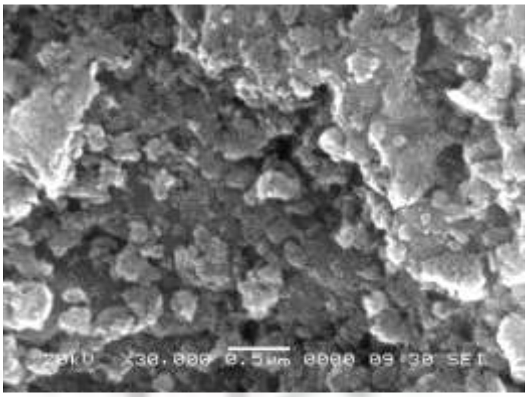

Figure 5. SEM image of hydrothermally synthesized (using 10M NaCl) TiO_2 thick film

Figure 5 depicts SEM image of hydrothermally synthesized TiO_2 using 10 M NaCl thick films, fired at 550°C. The grains are agglomerated. Effective surface to volume ratio is decreased and less number of oxygen ions are adsorbed as compared to the film in figure 4.

D. TEM Analaysis

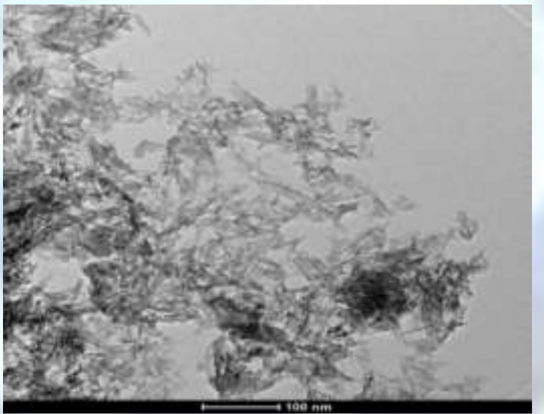

Figure 6(a). TEM image hydrothermally synthesized (using 5M NaCl) TiO_2 powder (X100 nm)

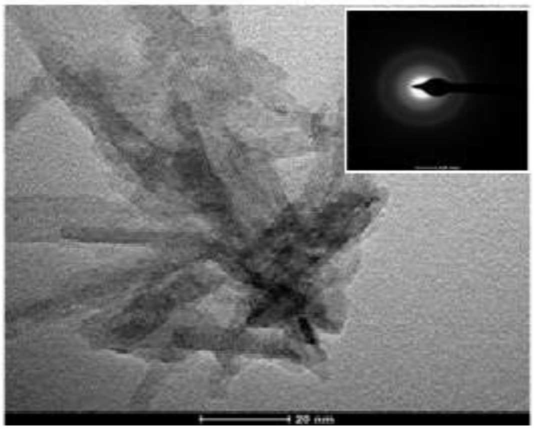

Figure 6(b). TEM image hydrothermally synthesized (using 5M NaCl) TiO_2 powder (X20 nm)

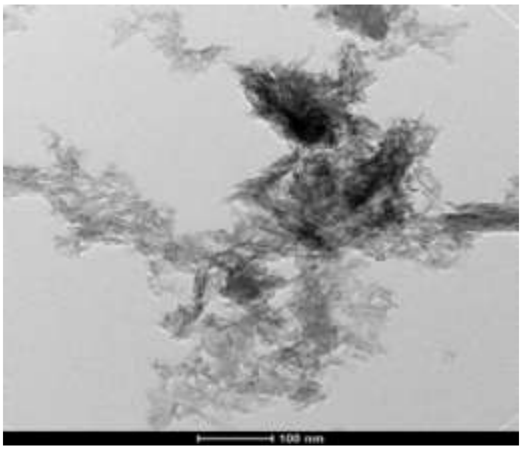

Figure 7(a). TEM image hydrothermally synthesized (using 10M NaCl) TiO_2 powder (X100 nm)

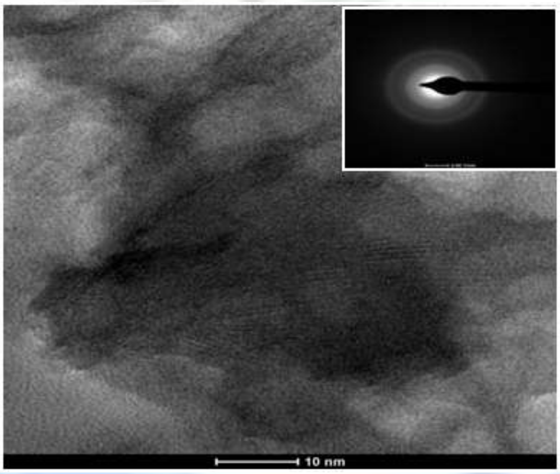

Figure:-7(b) TEM image hydrothermally synthesized (using 10M NaCl) TiO_2 powder (X10 nm)

Figure 6 (a) and 7(a) shows TEM images of hydrothermally synthesized TiO_2 powder using 5M NaCl and 10M NaCl at different magnification. Figure 6 (b) and 7 (b) shows magnified TEM image and selected area diffraction pattern; it reveals that TiO_2 is predominantly single crystalline anatase with lattice spacing of 0.324nm and 0.323nm respectively. The atoms are arranged in definite manner and TiO_2 powder is well crystalline.

E. IV Characteristics of TiO_2 Thick Films

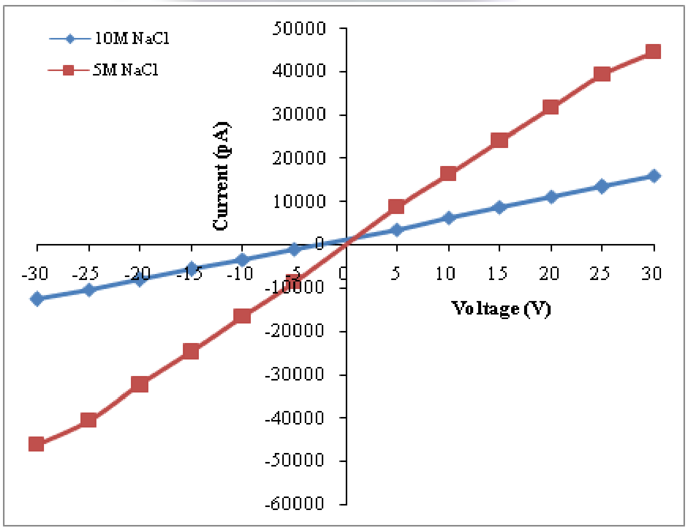

Figure 8. IV characteristics of TiO_2 thick films

Fig.8 I-V characteristics of TO_2 thick film are observed to be linear and symmetrical in nature, indicating the ohmic nature of silver contacts.

F. Variation of Conductivity of TiO_2 Thick Films

Figure 9 shows the dependence of conductivity of TiO_2 films with temperature in air and H_2S ambient. Electrical conductivity of these films goes on increasing with increase in temperature in air and gas (H_2S) ambient, indicating negative temperature coefficient (NTC) of resistance. This shows the semiconducting nature of the films. Slopes of the graphs between 50°C and 300°C are different for different curves.

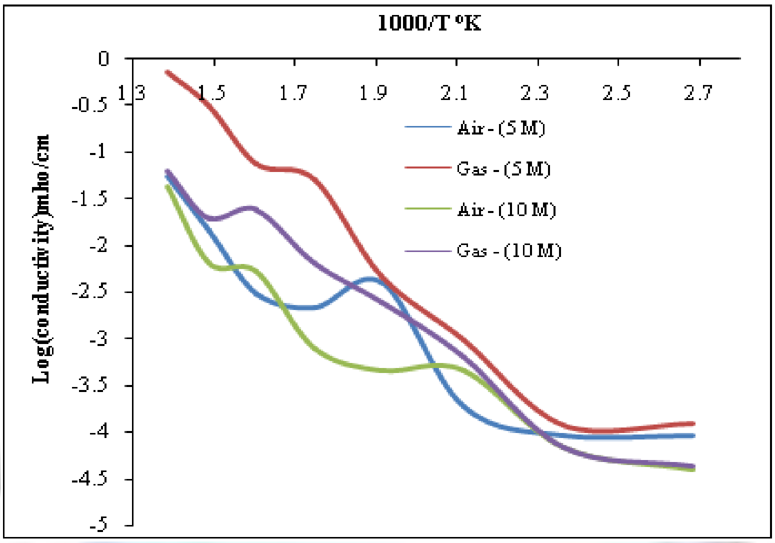

Figure 9. Electrical conductivity of hydrothermally synthesized (using 10M NaCl) TiO_2 thick films

G. Sensitivity of TiO_2 Thick Films for Various Operating Temperature

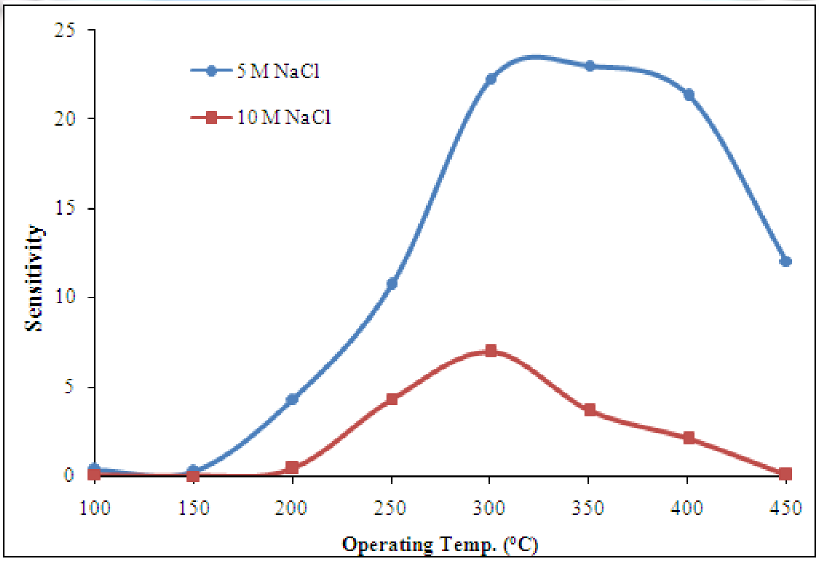

Figure 10. Sensitivity of TiO_2 thick films for various operating temperature

Figure 10 shows the variation in the sensitivity of H_2S gas (800 ppm) with operating temperatures. It is noted from the graph that response increases with increasing temperature, and attains a maximum at 350°C and decreases with further increase in operating temperature.

H. Selectivity of TiO_2 Thick Films for Various Gases

Figure 11 shows the histogram of the selectivity of TiO_2 thick film for various gases. The TiO_2 thick films were selective to H_2S gas against the other tested gases at 350°C.The sensitivity of thick films were 23 for H_2S gas.

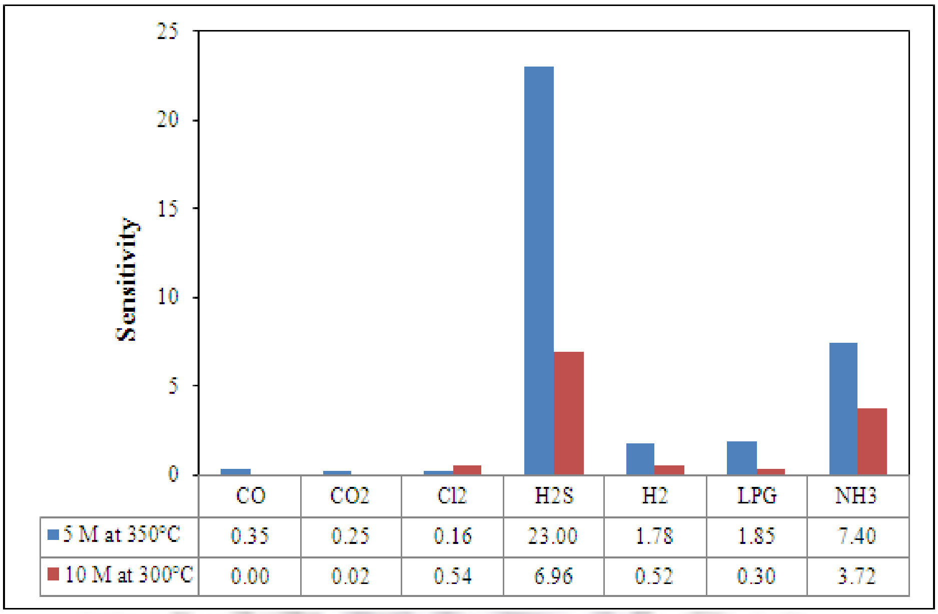

	CO	CO2	Cl2	H2S	H2	LPG	NH3
5 M at 350°C	0.35	0.25	0.16	23.00	1.78	1.85	7.40
10 M at 300°C	0.00	0.02	0.54	6.96	0.52	0.30	3.72

Figure 11. Selectivity of TiO_2 Thick Films for Various Gases

I. Role of Nanoparticles and nanorods in Gas Sensing Mechanism

Figure 12(a) and 12(b) represent the channel width in absence and on exposure of reducing gas respectively. When oxygen molecules are adsorbed on the particle surface, the conducting electrons from the surface particles are abstracted. The adsorbed O^- ions on the surface of particles scatter electrons existing within the Debye length δ. The depletion region is formed around the particles having depth δ and there would not be any electrons available for conduction. The effective channel width Lc becomes narrow. Lc can be written as, Lc = D- 2δ, where D is diameter of the particle under consideration. The initial resistance of the film, therefore, is very high in air ambient. If particle size is reduced up to nanolevel (<100nm), the channel would be almost blocked and the initial resistance would be infinite in air ambient.

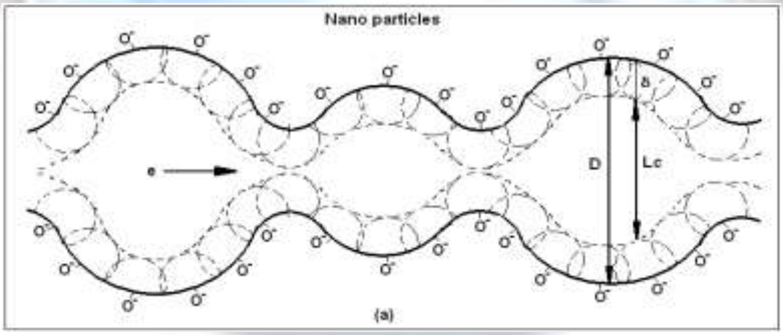

Figure 12(a). Model representing an adsorption of oxygen (in absence of target gas)

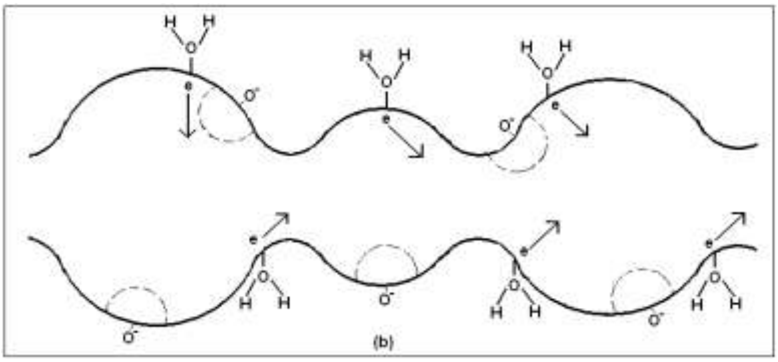

Figure 12(b). Broad conduction channel on exposure of target gas

On exposure of the reducing gas, the gas is oxidized and abstracted electrons are released increasing the channel width largely, that is, increasing the conduction of the film abruptly.

The nanocrystalline film offers grain sizes where the depletion layer has almost the same dimensions as the particle radii and consequently electrical conduction is predominantly grain controlled.

The following statements can be made regarding the role of nanomaterials in gas sensing.

- Gas sensor films, prepared from nanocrystalline powder, offer grain sizes, where the depletion layer has almost the same dimensions as the particle radii, and consequently electrical conduction is predominantly grain controlled.
- Porous films composed of nanoparticles with diameter between 6 and 20nm showed improved sensitivity and high gas selectivity due to increased surface area to volume ratio..
- Chemisorbed O^- species at the surface acts as scattering centers and resist the movement of charge carriers as represented schematically in Figure 12(a).
- Adsorption of reducing gas results in the decreased or elimination of these scattering centers as shown in Figure 12(b).
- When size of particles approaches that of Debye length, a clear decrease in the mobility of charge carriers' results. The effective increase in size of conduction channel leads to an increase in mobility.
- In particular, in our case, the diameter of the TiO_2 nanorods small and is comparable to the Debye length (about 27 nm at 1000 K). At this scale, the surface effect becomes more pronounced in charge carrier dynamics, and significantly changes the conductivity of the TiO_2 nanorods, resulting in enhanced gas sensing performance. The vertically aligned morphology of TO_2 nanowires provides not only a direct path for efficient electron collection but also a variety of channels for surface interactions between chemisorbed oxygen adions and reducing gases, which make more surface exposed to the testing gas than in the entangled nanowires. As a result, the sensing properties of TiO_2 nanoarrays were improved.

Acknowledgment

The authors are grateful to Dr. Dilip Dhondge Principal of K.T.H.M. College Nasik, Maharashtra, India for providing laboratory facilities. The authors are also thankful to Dr. V. B. Gaikwad, Director, B.C.U.D. Pune university for inspiring to do research.

References

[1]. T.Seiyama (Ed),Chemical Sensor Technology,1 and Elsevier,Amsterdam,1988,1990.
[2]. N.Yamazoe(Ed), Chemical Sensor Technology,3 and Elsevier,Amsterdam1991.
[3]. S.Yamauchi(Ed)Chemical Sensor Technology,4 and Elsevier,Amsterdam,1992.
[4]. W.Gopel,J.N.Hesse,J.N.Zemel(Eds.),Sensors,A ComperehensiveSurvey,vol.1-9,Wiley-VCH,Weinheim,1989-1995.
[5]. H.Baltes,W.Gopal,J.Hesse(Eds),Sensors Update,vol.1-5,Wiley-VCH,Weinheim,1996-1999.
[6]. G.Sberveglieri(Ed), Gas Sensors-Principles Operation and Developments, Kluwer Academic Pubishers,The Netherlands,1982.
[7]. N.Barsan,M.SchweizerBelberich,W.Gopal,Fresnius'J.Anal.Chem.365(1999)287-304.
[8]. S.sagtangelo,G.Messina,G.Faggio,A.Donato,L.De Luca,N.Donato,A.Bonavita,G.Neri,J.Solid State Chem,183(2010) 2451-2455.
[9]. D.Morris,R.G.Egdell,J.Mater.Chem.11(2001)3207-3210.
[10]. H.Tang , K . Prasad, R. Sanjines ,F. Levy ,TiO_2 anatase tine films as gas sensors , Sens. Actuators B 26-27 (1995)71-75.
[11]. H.Tang , H.Berger , P.E.Schmid , F.Levy , Optical properties of anatase TiO2, solid states commun.92(1994) 267-271
[12]. H.Tang , K . Prasad, R. Sanjines ,P.E.Schmid, F.Levy ,electrical and optical properties of TiO_2 anatase thin films , J.Appl.Phys.75(1994)2042-2047
[13]. S. K. Joshi, C. N. Rao, T. Tsuruto, S. Nagakura, New Materials, Narosa Publishing House (1992) Chap 1, 1-37.
[14]. P. T. Moseley, Thick film sensors (1994) 269.
[15]. B. Morten, J. Mater. Sci. 1 (1990) 118.
[16]. M. S. Setty, D. P. Amalnerkar, Thick film sensors, Ed. Prudenziati M. (Amsterdam: Elsevier, 1994).
[17]. T. Ishihara, Y. Nishi, H. Nishiguchi, Y. Takita, Detection mechnism of CuO-$BaTiO_3$ capacitive type CO sensor, in: Proceedings of ceramic sensors III, San Antonio, TX, USA, 6-11 October 1997.
[18]. Y.C.Zhang,H.Tagawa,S.Asakuwa,J.Mizusaki,H.Narita,Solid State Ionics 100(1997) 275.
[19]. Y. Noguchi, H. Koroiwa, M. Takita, Key Eng. Mater. 160 (1999) 79.
[20]. M.S. Wagh, L.A. Patil, D.P. Tanay Seth, Amalnerkar, Surface cupricated SnO_2–ZnO thick films as a H2S gas sensor, Mater. Chem. Phys. 84 (2004) 228–233.
[21]. S. D. Shinde, G. E. Patil, D. D. Kajale, V. B. Gaikwad and G. H. Jain, J. Alloys and Comp. 528, 109 (2012).
[22]. Ganesh E. Patil, D. D.Kajale, V. B.Gaikwad, N. K.Pawar and G. H. Jain, Sens. and Transducers Journal, 137, 47 (2012)
[23]. S. D.Shinde, G. E. Patil, D. D.Kajale, V. B.Gaikwad and G. H. Jain, Int. J. of Nanoparticles, 5, 126 (2012)
[24]. D. D. Kajale, G. E. Patil, V. B. Gaikwad, S. D. Shinde, D. N. Chavan, N. K. Pawar, S. R. Shirsath and G. H. Jain, Int. J. on Smart Sens. and Intelligent System, 5, 382 (2012)
[25]. N. K.Pawar, D. D.Kajale, G. E. Patil, V. G. Wagh, V. B.Gaikwad, M. K.Deore and G. H. Jain, Int. J. on Smart Sens. and Intelligent System, 5, 441 (2012)
[26]. Banfield, J.F., Veblen, D.R., Smith, D.J. Am. Mineral. Volume 76, page 343 (1991).
[27]. Banfield, J.F., Veblen, D.R., Smith, D.J. Am. Mineral. Volume 76, page 343 (1991).